Electrokinetic Transduction Of Acoustic Waves In Ocean Sediments

Gareth I. Block
Applied Research Laboratories, U.T. Austin
P.O. Box 8029
Austin, TX 78713-8029
phone: (512) 835-3855 fax: (512) 835-3259 e-mail: gblock@arlut.utexas.edu

Nicholas P. Chotiros
Applied Research Laboratories, U.T. Austin
P.O. Box 8029
Austin, TX 78713-8029
phone: (512) 835-3512 fax: (512) 835-3259 e-mail: chotiros@arlut.utexas.edu

Grant Number: N00014-02-1-0335
http://www.arlut.utexas.edu/

LONG-TERM GOALS

Our long-term goal is to understand the deformation behavior of saturated granular media under various load conditions. These materials are found to be hierarchical, with additional length scales embedded in the macroscopic equations used to describe them. We are also focused on gathering experimental data to support this modeling effort.

OBJECTIVES

Our specific objectives are to develop models of ocean sediments that reveal the multi-scale aspects of sediment response. Frequency-dependent acoustic behavior is derived from macroscopic parameters, and these parameters in turn depend on microscopic features that characterize the material. In particular, this project details how electrokinetic phenomena—which have been used in seismology to characterize consolidated porous media—are directly coupled to wave motion. In support of this research, we have developed EK transduction techniques for studying unconsolidated sediments.

APPROACH

Multi-scale homogenization methods (Burridge and Keller [1]; Auriault [2]; Cushman [3]) and volume-averaging methods (Slattery [4,5]; Pride [6]) were introduced to explain the exact process by which microscopic variations in porous media can be homogenized to produce macroscopic field equations. Both of these approaches show that Biot theory [7] relies on a separation of length scales, and that the governing equations necessarily regard fluid and solid phases as *coincident* on the macroscale (that is, each macroscopic material point is composed of both fluid and solid phases), as in Figure 1. Volume-averaging methods require the acoustic wavelength λ to be much larger than the linear size L of the Representative Elementary Volume (REV) over which averaging takes place. Moreover, L ought to be much larger than the characteristic size of the pores d so that a suitable average can be taken.

Report Documentation Page

Form Approved
OMB No. 0704-0188

1. REPORT DATE	2. REPORT TYPE	3. DATES COVERED
30 SEP 2003		**00-00-2003 to 00-00-2003**

4. TITLE AND SUBTITLE
Electrokinetic Transduction Of Acoustic Waves In Ocean Sediments

5a. CONTRACT NUMBER
5b. GRANT NUMBER
5c. PROGRAM ELEMENT NUMBER

6. AUTHOR(S)

5d. PROJECT NUMBER
5e. TASK NUMBER
5f. WORK UNIT NUMBER

7. PERFORMING ORGANIZATION NAME(S) AND ADDRESS(ES)
Applied Research Laboratories, U.T. Austin,,P.O. Box 8029,,Austin,,TX,78713

8. PERFORMING ORGANIZATION REPORT NUMBER

9. SPONSORING/MONITORING AGENCY NAME(S) AND ADDRESS(ES)

10. SPONSOR/MONITOR'S ACRONYM(S)
11. SPONSOR/MONITOR'S REPORT NUMBER(S)

12. DISTRIBUTION/AVAILABILITY STATEMENT
Approved for public release; distribution unlimited

13. SUPPLEMENTARY NOTES

14. ABSTRACT
Our long-term goal is to understand the deformation behavior of saturated granular media under various load conditions. These materials are found to be hierarchical, with additional length scales embedded in the macroscopic equations used to describe them. We are also focused on gathering experimental data to support this modeling effort.

15. SUBJECT TERMS

16. SECURITY CLASSIFICATION OF:			17. LIMITATION OF ABSTRACT	18. NUMBER OF PAGES	19a. NAME OF RESPONSIBLE PERSON
a REPORT	b ABSTRACT	c THIS PAGE			
unclassified	**unclassified**	**unclassified**	**Same as Report (SAR)**	**9**	

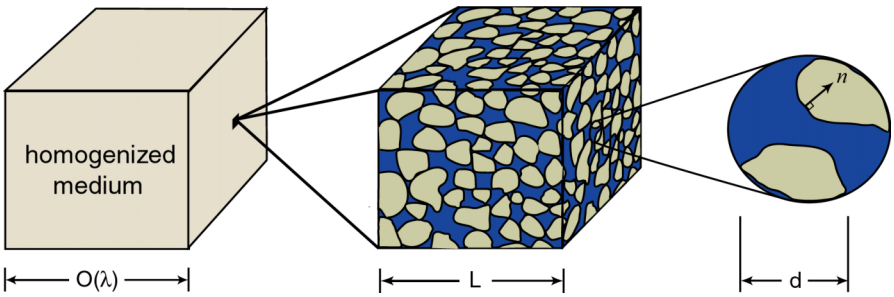

Figure 1. Hierarchical model implicit in homogenization. From left to right: (a) at the macroscopic scale, both phases are coincident when the medium is homogenized, (b) each material point consists of a volume cell made up of resolvable grains whose properties and dynamics are averaged over, and (c) the wall normal vector, n, at the solid interface.

These constraints result in the triple inequality under which Biot theory can be applied: $\lambda >> L >> d$. (For many ocean sediments, this sets a maximum operating frequency of about 1 MHz.) The moving average of a microscopic field B is defined by

$$\overline{B}(\mathbf{r}) := \frac{1}{V}\int_{V(\mathbf{r})} B(\mathbf{r}')dV(\mathbf{r}). \tag{1.1}$$

Suppress the ***r***-dependence for the present. The "averaging theorem" due to Slattery [4] is the rule by which spatial derivatives and averaging are interchanged:

$$\nabla\overline{B} = \overline{\nabla B} - \frac{1}{V}\int_S \mathbf{n}B(\mathbf{r}')dS. \tag{1.2}$$

Both Equations (1.1) and (1.2) are used to average the microscopic fluid and solid constitutive relations and equations of motion. Within the averaging volume, boundary conditions that arise between the two microscopic phases lead naturally to interfacial coupling (the surface integral over S, the internal phase interface, in Equation (1.2)) that act as sources of "accumulated" drag or heat transfer in the macroscopic equations.

WORK COMPLETED

We have implemented a numerical model of the following coupled EK-Biot theory. The bulk density ρ_{bulk} and stress tensor $\boldsymbol{\tau}_{bulk}$ are defined in terms of the fluid and solid densities, ρ_f and ρ_s, and averaged stresses, $\overline{p}$ and $\overline{\boldsymbol{\tau}}_s$, respectively.

$$\begin{aligned}\rho_{bulk} &= (1-\phi)\rho_s + \phi\rho_f,\\ \boldsymbol{\tau}_{bulk} &= (1-\phi)\overline{\boldsymbol{\tau}}_s - \phi\overline{p}\mathbf{I}.\end{aligned} \tag{2.1}$$

For a homogeneous, isotropic material, the linearized conservation of bulk momentum is written in terms of the averaged fluid $\overline{\mathbf{u}}_f$ and solid $\overline{\mathbf{u}}_s$ displacements (assuming the fields to be time-harmonic):

$$-\omega^2\left[\left(1-\phi\right)\rho_s\bar{\mathbf{u}}_s+\phi\rho_f\bar{\mathbf{u}}_f\right]=\nabla\cdot\boldsymbol{\tau}_{bulk}, \tag{2.2}$$

where the fluid volume fraction and angular frequency are denoted by ϕ and ω, respectively. The frequency dependent permeability $k(\omega)$ appears in a generalized form of Darcy's law that relates the gradient of the pore pressure (and acceleration of the pore walls) to the relative fluid velocity. In terms of the relative fluid displacement, $\bar{\mathbf{w}}=\phi\left(\bar{\mathbf{u}}_f-\bar{\mathbf{u}}_s\right)$,

$$-i\omega\bar{\mathbf{w}}=\frac{k(\omega)}{\mu}\left(-\nabla\bar{p}+\rho_f\omega^2\bar{\mathbf{u}}_s\right), \tag{2.3}$$

where μ is the fluid viscosity. Biot described the effects of frequency on pore fluid motion by noting that Poiseuille (parabolic) flow in the pores transitions to an acoustic boundary layer near the pore wall as the frequency increases beyond a critical value (thought to lie between 1 – 10 kHz for medium-grain sands). The dynamic permeability $k(\omega)$ captures this transition; it is related to the "accumulated" drag over the microscopic fluid-solid interface within an averaging cell.

Conservation of energy is derived similarly, leading to an equation for the bulk temperature field under the assumption of local thermal equilibrium (Slattery [5]):

$$\left[\phi\rho_f c_{Vf}+\left(1-\phi\right)\rho_s c_{Vs}\right]\frac{\partial T_{bulk}}{\partial t}=-\nabla\cdot\bar{\mathbf{q}}_{eff}+Q_{source}, \tag{2.4}$$

where c_{Vf} and c_{Vs} are the specific heats at constant volume, and the effective heat flux

$$\begin{aligned}\bar{\mathbf{q}}_{eff}&=-\left[\phi\hat{k}_f+\left(1-\phi\right)\hat{k}_s\right]\nabla T_{bulk}-\bar{\mathbf{h}}\\&=\left(\hat{k}_{stag}+\hat{k}_{disp}\right)\nabla T_{bulk},\end{aligned} \tag{2.5}$$

where the $\hat{k}_f$ and $\hat{k}_s$ are the fluid and solid thermal conductivities, respectively. The thermal tortuosity $\bar{\mathbf{h}}$—a source term related to heat transfer between phases on the microscopic level—can be related to "stagnant" ($\hat{k}_{stag}$) and "dispersive" ($\hat{k}_{disp}$) heat transfer. Thermal dispersion depends on the fluid velocity and is important for high-speed flow (Angirasa and Peterson [8]). Current work assumes these nonlinearities to be second order. Equation (2.4) ignores thermal convection and only the stagnant, nondispersive case is treated. This leads to *uncoupled thermoelasticity*: for a given heat source, Q_{source}, the temperature field can be calculated prior to the other mechanical fields. Subsequently, gradients of the fluid and solid thermal stresses act as source terms in Equations (2.2) and (2.3). These stresses are given by

$$\begin{aligned}p_{TH}&=\phi\beta_f K_f T_{bulk},\\\boldsymbol{\tau}_{s,TH}&=-\left(1-\phi\right)\beta_s K_s T_{bulk}\mathbf{I},\end{aligned} \tag{2.6}$$

where K_f, K_s, and β_f, β_s are fluid and solid elastic moduli and coefficients of thermal expansion, respectively.

Electrokinetics describes how the pore fluid and grain surface chemistry affect relative fluid motion. This has been used to great advantage to study wave propagation and material behavior in saturated, poroelastic media (see Beamish [9]; Mikhailov *et al.* [10]; Pengra *et al.* [11]). The theory we use relies on Pride [6], who derived an extended form of Biot theory that couples Maxwell's equations to the fluid and solid governing equations at the microscale. Here we simply note that the generalized Darcy's law in Equation (2.3) must be modified to include the average electric field $\overline{\mathbf{E}}$, current density $\overline{\mathbf{J}}$, and bulk conductivity σ_{bulk}:

$$-i\omega\overline{\mathbf{w}} = \frac{k(\omega)}{\mu}\left(-\nabla\overline{p} + \rho_f\omega^2\overline{\mathbf{u}}_s\right) + L(\omega)\overline{\mathbf{E}}, \tag{2.7}$$

$$\overline{\mathbf{J}} = L(\omega)\left(-\nabla\overline{p} + \rho_f\omega^2\overline{\mathbf{u}}_s\right) + \sigma_{bulk}\overline{\mathbf{E}}. \tag{2.8}$$

Equation (2.8) is an extension of Ohm's law. The off-diagonal terms, $L(\omega)$, are generally equal, and transition from a constant value at low frequencies to a smaller, high frequency value. It turns out that EK-Transmission "transduction" efficiencies can be much greater than 1 Pascal per Volt. It has therefore been possible to generate large EK pressures with an applied high voltage source, and to use these EK-pressure waves to study the poroelastic properties of ocean sediments in the laboratory.

Since FY02, we have designed and built a working EK-Transmission apparatus to generate sound waves and measure the electrical and mechanical properties of sediments. Our first step was to prepare solutions of NaCl and de-ionized water with various resistivities. Medium-grain silica sand with a nominal diameter of 250 – 300 microns (sand blasting sand) was boiled for a short time to dissipate gas bubbles trapped in the sediment. A gold-plated electrode assembly approximating a dipole with 1.5 cm separation distance was attached to a high voltage power supply and capacitor bank. This dipole delivers the applied electric field, $\mathbf{E}_{app}(\mathbf{r},t)$, used in our modeling. The electrical current causes ionic convection currents (driving EK phenomena) and dissipates energy in the form of heat (Joule heating). To model the acoustic response caused by Joule heating, the applied power density $\sigma_{bulk}\left|\mathbf{E}_{app}\right|^2$ is used as the additional source in Equation (2.4). The resulting averaged thermal stresses, along with the applied current source $\overline{\mathbf{C}}$, are input into the Green state formulation of the EK-Biot system (based on Haartsen and Pride [12]). Displacement fields generated from this formulation are used to calculate the far field pressure time-series due a physical dipole in close approximation to the experiment.

A PZT acoustic transducer was buried about 15 cm from the electrode, amplified by a 40 dB preamplifier, and attached to a computerized DAQ system synchronized to the high voltage supply. The input current to the electrodes was also monitored. The combined effects of the capacitor bank and varying resistance of each NaCl solution introduced a natural timescale (of a few microseconds) over which the input current decayed to zero. Figure 2 shows an example of the experimental apparatus and measured time-series for one NaCl solution.

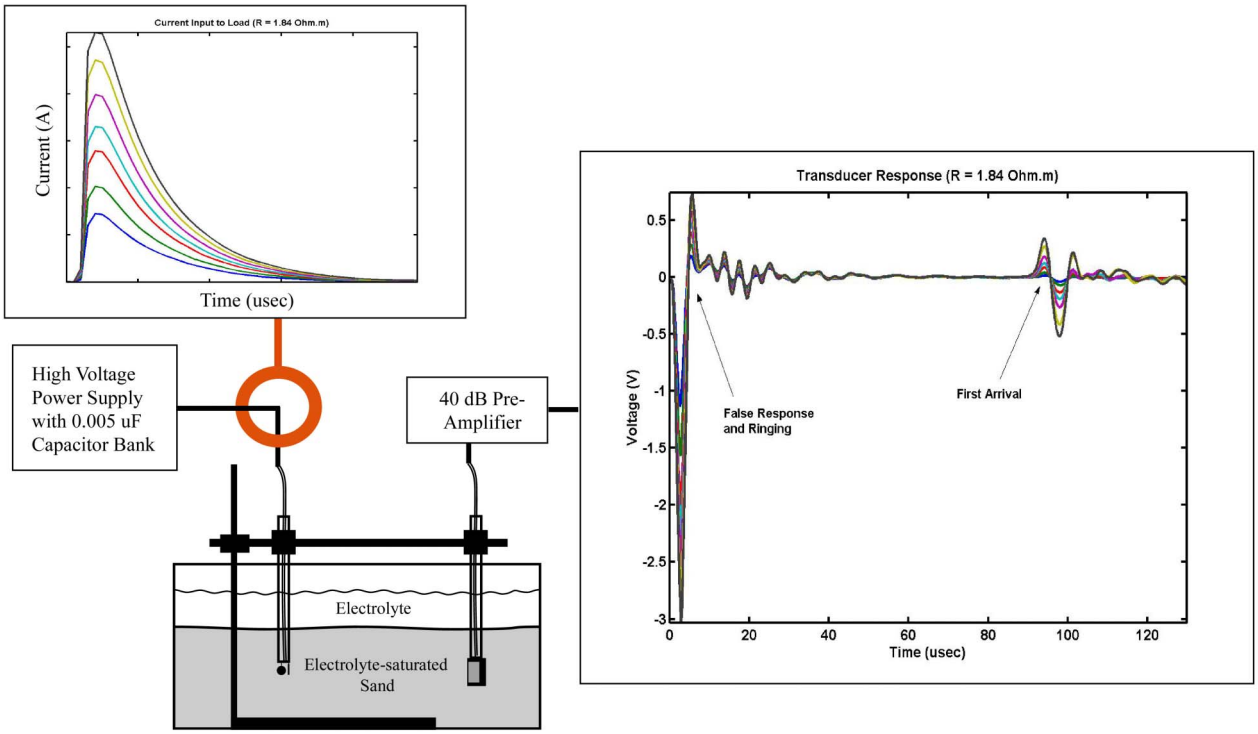

Figure 2. EK-Transmission apparatus and measured pressure. A high voltage power supply is routed through a capacitor bank and current measuring loop, as well as through a buried dipole electrode. In this example of real time-series data, the pressure measured by the buried hydrophone (about 15 cm from the electrode apparatus) shows a characteristic arrival signature for a range of applied voltages.

RESULTS

Our first approach has been to simply compare the peak of the input current to the peak of the first arrival. Thus we tabulated the dependence of the measured pressure on the applied current in the form of a power law, $p_{meas} = a(\sigma_{bulk})I_{app}^{m}$. When both EK and thermoelastic pressures are present in the measured signal, the exponent *m* depends on the current I_{app}:

$$p_{meas} = a_{EK} I_{app} + a_{TH} I_{app}^{2} \approx a I_{app}^{m}, \qquad (3.1)$$

where $1 \le m \le 2$. The EK-Biot and energy equations predict that the coefficients for electrokinetic a_{EK} and thermal a_{TH} pressure (as well as the "effective" term, *a*) depend on the bulk electrical conductivity (inverse of the resistivity, which is used in the subsequent plots). Our modeling generates both EK and thermal pressures over the experimental range of applied currents. These numerical "data points" are used to create a power law relation between pressure and applied current. Thus the exponent *m* is both measured and predicted numerically in the same way.

In the top panel of Figure 3, pressures measured for the EK-Transmission experiment performed in salt water are shown on a log-log plot. For each set of applied voltages and salt solutions, the pressure

showed a quadratic dependence on applied current (see legend for slopes of each curve). The resistivity of the pore fluid increases as green transitions to blue. As only a thermoelastic response is present in the water experiment, the exponent $m \approx 2$ is expected for all resistivities. The data for the same experiment in unconsolidated sediment is shown in the bottom panel of Figure 3. In this case, we note that the exponent m varies between 1.39 and 1.84 as the resistivity is decreased. Thus the preliminary data suggests that a transition occurs between EK and thermoelastic regimes.

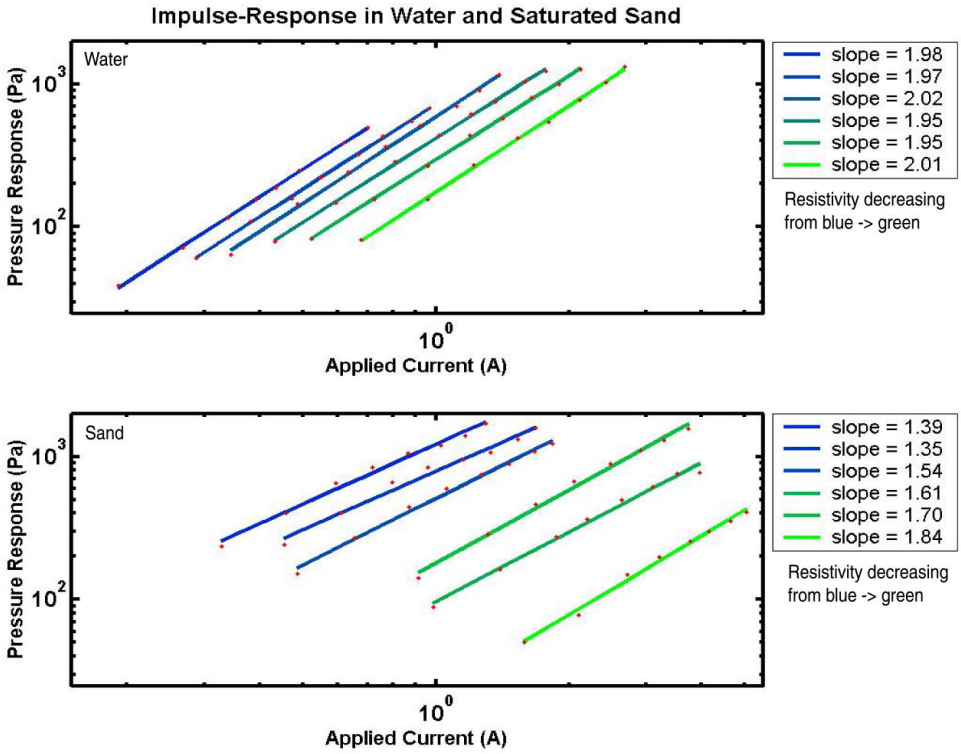

Figure 3. Impulse-Response of Water and Electrolyte-Saturated Sand. The measured pressure in salt water shows a simple quadratic dependence on applied current over a resistivity range of 0.5 – 5.0 Ωm (the power law exponent is a constant value of 2). In the electrolyte-saturated sediment, the power law varies between 1.35 and 1.84 as the resistivity decreases (from blue to green). The slopes of each power-law fit to the data are shown in the legends.

The numerical predictions in Figure 4 match the qualitative features of the preliminary experimental data. Predictions are shown for three values of the DC permeability of the sediment. For the smallest permeability, $k = 10^{-12} m^2$ (characterizing fine-grain sand), the EK response is strong enough to produce values of the exponent m near unity. Each of these curves shows that the power law exponent increases monotonically from values characteristic of an EK regime to values characteristic of a thermoelastic regime. Current work focuses on gathering more data to support this trend, as well as the development of new methods for comparing measurements to numerical predictions.

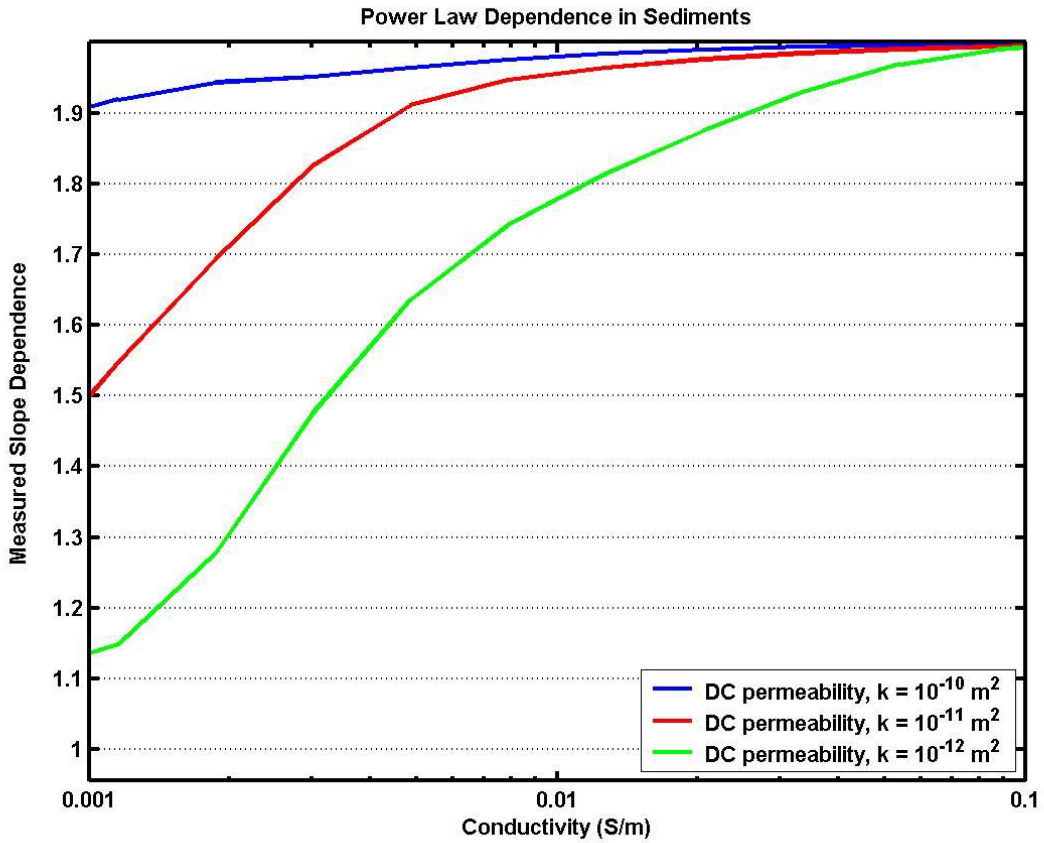

Figure 4. Numerically predicted power law dependence in saturated sand. The predicted dependence of pressure on applied current is characterized by a power law exponent, m, plotted against conductivity for various DC permeabilities. The curves for each permeability increase from above 1 and asymptote at a value of 2.

IMPACT/APPLICATIONS

EK generation and reception of acoustic waves may yield new methods of measuring the material properties of the sea floor. Using the coupled EK-Biot model already described, we might use EK techniques to determine properties of ocean sediments such as permeability, volume fraction and tortuosity *in situ*. These Biot parameters are critically important and difficult to measure. Other models that reliably predict wave propagation in *non-Biot* granular materials, extended to include EK phenomena, may also yield properties of the sediment microstructure. These are new capabilities that we currently do not possess. They will have a significant impact on our ability to model sound propagation and penetration into the seabed in applications involving Anti-Submarine Warfare, Mine Counter-Measures, and sonar performance models. Similarly, ocean environmental models (used in tandem with acoustic inversion) can be checked and corrected as necessary.

TRANSITIONS

No transitions have been made at this time.

RELATED PROJECTS

The multi-scale approach described here is being extended to include other aspects of heterogeneous deformation. We have been studying stochastic variability in poroelastic media, as viewed from both the macroscopic level (where the permeability, for example, might vary over centimeters or meters) and the microscopic level (where we use ensemble averaging to produce the macroscopic, poroelastic equations).

REFERENCES

1. Burridge, R. and Keller, J. B., 1981. Poroelasticity equations derived from microstructure: *J. Acoust. Soc. Am.*, **70:** 1140 – 1146.
2. Auriault, J. L., 1994. Deformable porous media with double porosity. Quasi-statics I: coupling effects, Quasi-statics II: memory effects, III: acoustics: Transport in Porous Media, **7, 10, 14**: 63 – 82, 153 – 169, 143 – 162.
3. Cushman, J.H., 1997. The Physics of Fluids in Hierarchical Porous Media: Angstroms to Miles: Kluwer Academic Press.
4. Slattery, J. C., 1967. Flow of viscoelastic fluids through porous media: *Am. Ch. Eng. Journal*: 1066 – 1071.
5. Slattery, J. C., 1981. Momentum, energy, and mass transfer in continua: R.E. Krieger Publishing Company, New York.
6. Pride, S., 1994. Governing equations for the coupled electromagnetics and acoustics of porous media: *Phys. Rev. B*, **50** (21): 15678 – 15696.
7. Biot, M. A., 1956. Theory of propagation of elastic waves in a fluid-saturated porous solid. I. Low-frequency range and II. Higher frequency range: *J. Acoust. Soc. Am.*, **28**: 168 – 178, 179 – 191.
8. Angirasa, D. and Peterson, G. P., 1999. Forced convection heat transfer augmentation in a channel with a localized heat source using fibrous material: *ASME J. Electronic Packaging*, **121**: 1 – 7.
9. Beamish, D., 1999. Characteristics of near-surface electrokinetic coupling: *Geophys. J. Int.*, **137**: 231 – 242.
10. Mikhailov, O.V., Haartsen, M.W. and Toksoz, M.N., 1997. Electroseismic investigation of the shallow subsurface: field measurements and numerical modeling: *Geophysics*, **62**: 97 – 105.
11. Pengra, D.B., 1999. Determination of rock properties by low-frequency AC electrokinetics: *J. Geophys. Res.*, **104** (B12): 29485 – 29508.
12. Haartsen, M.W. and Pride, S.R., 1997. Electroseismic waves from point sources in layered media: *J. Geophys. Res.*, **102** (B11): 24745 – 24769.

PUBLICATIONS

1. Harris, J.G. and Block, G., 2003. The coupling of elastic, surface-wave modes by a slow, interfacial inclusion: *J. Acoust. Soc. Am*, submitted for publication.
2. Block, G., 2003. Coupled electrokinetic-Biot theory and measurement techniques in sediment acoustics: *16th ASCE Engineering Mechanics Conference Proceedings, July 16 – 18, 2003: University of Washington, Seattle*.

PATENTS

No patents have been awarded at this time.

HONORS/AWARDS/PRIZES

Gareth Block, ARL:UT, was awarded second prize in the "Student Best Paper Award" at the Acoustical Society of America conference in Cancun, Mexico, November 2002.